

LIMITS OF SEQUENCES OF PSEUDO-ANOSOV MAPS AND OF HYPERBOLIC 3-MANIFOLDS

SYLVAIN BONNOT, ANDRÉ DE CARVALHO, JUAN GONZÁLEZ-MENESES, AND TOBY HALL

ABSTRACT. There are two objects naturally associated with a braid $\beta \in B_n$ of pseudo-Anosov type: a (relative) pseudo-Anosov homeomorphism $\varphi_\beta: S^2 \rightarrow S^2$; and the finite volume complete hyperbolic structure on the 3-manifold M_β obtained by excising the braid closure of β , together with its braid axis, from S^3 . We show the disconnect between these objects, by exhibiting a family of braids $\{\beta_q : q \in \mathbb{Q} \cap (0, 1/3]\}$ with the properties that: on the one hand, there is a fixed homeomorphism $\varphi_0: S^2 \rightarrow S^2$ to which the (suitably normalized) homeomorphisms φ_{β_q} converge as $q \rightarrow 0$; while on the other hand, there are infinitely many distinct hyperbolic 3-manifolds which arise as geometric limits of the form $\lim_{k \rightarrow \infty} M_{\beta_{q_k}}$, for sequences $q_k \rightarrow 0$.

1. INTRODUCTION

This article presents a somewhat surprising phenomenon on the interface between the theories of surface homeomorphisms and of 3-manifold geometry. Two theorems due to Thurston associate to certain mapping classes on a surface — the pseudo-Anosov mapping classes — two different types of canonical objects.

- The Classification Theorem for Surface Homeomorphisms [22, 11, 6] states that every irreducible mapping class which is not of finite order contains a pseudo-Anosov homeomorphism, which is unique up to topological conjugacy. Such a mapping class is said to be of pseudo-Anosov type.
- The Hyperbolization Theorem for Fibered 3-Manifolds [23, 19, 17] states that the mapping torus of a mapping class admits a complete hyperbolic metric of finite volume (unique up to isometry by the Mostow-Prasad Theorem) if and only if the mapping class is of pseudo-Anosov type.

In this paper we consider mapping classes of marked spheres, represented by elements of Artin's braid groups: an n -braid $\beta \in B_n$ defines a mapping class on the n -marked disk, and hence on the $(n + 1)$ -marked sphere. We say that β is of pseudo-Anosov type if and only if the corresponding mapping class is, and in this case we can associate to it:

- a homeomorphism $\varphi_\beta: S^2 \rightarrow S^2$, unique up to conjugacy, which is pseudo-Anosov relative to the marked points (that is, whose invariant foliations are permitted to have 1-pronged singularities at these points); and

Date: January 2019.

The authors are grateful for the support of FAPESP grant 2016/25053-8 and CAPES grant 88881.119100/2016-01. AdC is partially supported by CNPq grant PQ 302392/2016-5. JGM is partially supported by Spanish Project MTM2016-76453-C2-1-P and FEDER.

- the hyperbolic 3-manifold¹ $M_\beta = S^3 \setminus (\bar{\beta} \cup A)$ — where $\bar{\beta}$ is the closure of β and A is its braid axis — which is homeomorphic to the mapping torus of φ_β (acting on the sphere punctured at the $n + 1$ marked points).

We will present a family of pseudo-Anosov braids $\{\beta_q : q \in \mathbb{Q} \cap (0, 1/3]\}$, with $\beta_{m/n} \in B_{n+2}$, with the following properties:

- The pseudo-Anosov homeomorphisms $\varphi_q := \varphi_{\beta_q} : S^2 \rightarrow S^2$ can be normalized in such a way that $\varphi_q \rightarrow \varphi_0$ as $q \rightarrow 0$, where φ_0 is a fixed sphere homeomorphism (the *tight horseshoe map*, derived from Smale’s horseshoe map).
- The hyperbolic 3-manifolds $M_q := M_{\beta_q}$ have the property that there are infinitely many distinct finite volume hyperbolic 3-manifolds which can be obtained as geometric limits $\lim_{k \rightarrow \infty} M_{q_k}$ for some sequence $q_k \rightarrow 0$.

The braids β_q are the *NBT braids* of [15]: they are pseudo-Anosov braids for which the corresponding pseudo-Anosov homeomorphisms φ_q have particularly simple train tracks (see Remark 5). The fact that $\varphi_q \rightarrow \varphi_0$ as $q \rightarrow 0$ is a straightforward consequence of results of [5]: the main content of this paper is an analysis of possible geometric limits of sequences M_{q_k} .

The principal technique which we will use is Dehn surgery, and we now briefly recap some key definitions and results, in order to fix conventions (which are taken from section 9 of Rolfsen’s book [20]). Let $L = L_1 \cup \dots \cup L_n$ be a link in S^3 with components L_i , and let N be a closed tubular neighborhood of L_1 which is disjoint from the other components of L . Pick a basis $([\mu], [\lambda])$ for $H_1(\partial N, \mathbb{Z})$ such that the ‘meridian’ μ is contractible in N and the ‘longitude’ λ has linking number 0 with L_1 .

If J is a homotopically non-trivial simple closed curve in ∂N , then we can construct a 3-manifold

$$M = S^3 \setminus (L \cup \overset{\circ}{N}) \cup_h N,$$

where $h: \partial N \rightarrow \partial N$ is a homeomorphism which takes μ onto J . Writing $[J] = b[\mu] + a[\lambda]$, we say that M is obtained from $S^3 \setminus L$ by *Dehn filling L_1 with surgery coefficient $r = b/a$* : this definition is independent of the choices of orientations of μ , λ and J . (This corresponds to Dehn filling coefficient (b, a) in the notation used by SnapPy [7], where the coefficients (b, a) and $(-b, -a)$ lead to the same surgery. We will always assume that a and b are coprime.) In particular, setting $r = \infty$ if and only if $[J] = \pm[\mu]$, i.e., $b = 1$ and $a = 0$, then $M = S^3 \setminus (L_2 \cup \dots \cup L_n)$: filling L_1 with surgery coefficient ∞ is the same as erasing the component L_1 from the link L .

Suppose now that we have assigned surgery coefficients to some of the components of L , and that L_1 is an unknotted component of L . Applying a positive meridional twist to the (solid torus) complement of a tubular neighborhood of L_1 is referred to as *performing a +1 twist on L_1* : if D is a disk bounded by L_1 which the other components of L intersect transversely, then the effect of this twist on the link L is to replace each segment of L which intersects D with a helix which screws through a collar of D in the right-handed sense. If $t \in \mathbb{Z}$, then *performing a t twist on L_1* means performing t such twists if $t \geq 0$, or $-t$ left-handed twists if $t < 0$.

¹All of the 3-manifolds in this paper are of the form M_β for some pseudo-Anosov braid β , and we consider them as hyperbolic 3-manifolds without further comment.

The revised link L' after a t twist on L_1 describes the same 3-manifold as L provided that the surgery coefficients (on those components of L which have them) are updated using the formulæ:

$$(1) \quad \begin{aligned} r_1(L_1) &= \frac{1}{t + 1/r_0(L_1)}, \\ r_1(L_i) &= r_0(L_i) + t(\text{lk}(L_1, L_i))^2 \quad (i > 1), \end{aligned}$$

where $r_0(L_i)$ and $r_1(L_i)$ are the surgery coefficients on L_i before and after the twist, and $\text{lk}(L_1, L_i)$ is the linking number of L_1 with L_i .

In this paper, we will only perform twists in the case where $L = \bar{\beta} \cup A$ is the closure of a braid together with its axis; and we will only perform them on either the braid axis A or a fixed component of $\bar{\beta}$ (one which corresponds to a single string of the braid). It will therefore be convenient to describe the effects of such twists directly on the braid.

- (a) A t -twist on the braid axis A replaces β with $\beta\theta^{-t}$, where θ is a full twist in the braid group.
- (b) Figure 1 (a) is a schematic representation of $\bar{\beta} \cup A$, where β has a fixed string which links one of the other strings. The effect of a -1 twist on the corresponding component of $\bar{\beta}$ is shown in (b), which is followed by a conjugacy to obtain the braid of (c). Because this braid has the same structure as β , the process can be repeated $t - 1$ more times to obtain the braid of (d), which is the effect of applying a $-t$ twist on the fixed string. It has t more strands than β .

We shall also consider twists on fixed strings which link a ribbon of other parallel strings of the braid. Figure 2 shows the effect of a $-t$ twist in this case, determined analogously. If the ribbon consists of m strings, then this increases the number of strings of β by tm .

In order to carry out a $+t$ twist on a fixed string, we will conjugate β to take the form of the right hand side of Figure 2. The $+t$ twist will then reduce it to the braid on the left hand side.

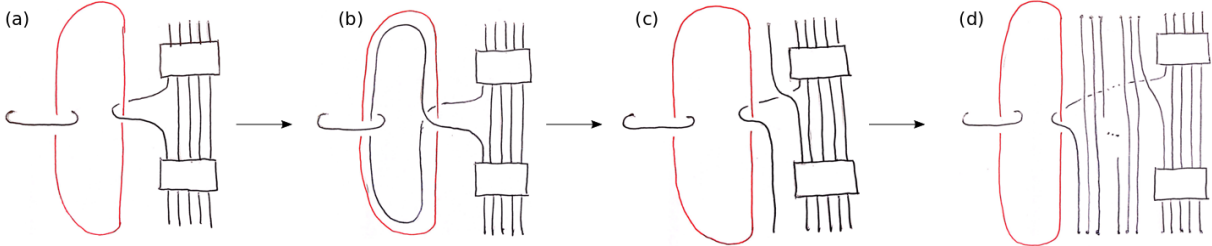


FIGURE 1. -1 and $-t$ twists on a fixed string which links one other string.

We will use the following simplified version of Thurston's Hyperbolic Dehn Surgery Theorem, which follows from Chapters 4 and 5 of [24], see also [1, 18].

Theorem 1. *Let $L = L_1 \cup \dots \cup L_n$ be a link in S^3 such that $M := S^3 \setminus L$ is a complete hyperbolic 3-manifold of finite volume, $r_i = b_i/a_i$ be a sequence of rationals with $a_i^2 + b_i^2 \rightarrow \infty$, and M_i be the sequence of 3-manifolds obtained by Dehn filling L_1 with surgery coefficients r_i . Then M_i converges geometrically to M , and the convergence is non-trivial in the sense that M_i and M are distinct for all i , so that there are infinitely many distinct 3-manifolds M_i .*

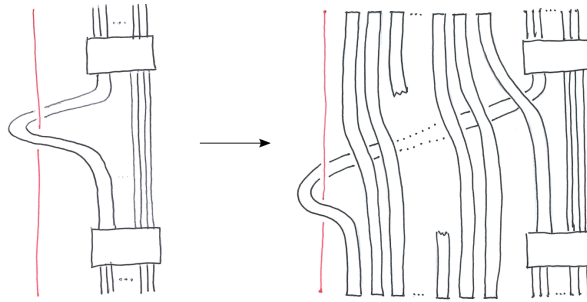


FIGURE 2. A $-t$ twist on a fixed string which links a ribbon of parallel strings.

2. THE BRAIDS β_q

Recall that the *positive permutation braid* $\beta \in B_n$ defined by a permutation $\pi \in S_n$ is the unique n -braid which induces the permutation π on its strings, and which has the properties that every pair of strings crosses at most once, and that every crossing is in the positive sense (we adopt the convention, following Birman [3], that a braid crossing is positive if the left string crosses over the right one). Thus a diagram of β can be constructed by drawing the first to the n^{th} strings in order, with the i^{th} string going from position i to position $\pi(i)$ and passing underneath any intervening strings which have already been drawn.

The following definition is from theorem 2.1 of [15], and the fact that the braids defined are of pseudo-Anosov type is contained in the proof of theorem 2.3 of the same paper. (There the braids β'_q are also defined for $q \in (1/3, 1/2)$, but this is done in a different way and, since we are only interested in limits as $q \rightarrow 0$, is not relevant here.) Here and throughout the paper, when we write a positive rational number as m/n , we will always assume that m and n are coprime and positive.

Definition 2 (The braids β'_q). Let $q = m/n \in \mathbb{Q} \cap (0, 1/3]$. The braid $\beta'_q \in B_{n+2}$ is the positive permutation braid (see Figure 3) defined by the cyclic permutation

$$(2) \quad \pi_q(r) = \begin{cases} r + m & \text{if } 1 \leq r \leq n - 3m + 1, \\ r + m + 1 & \text{if } n - 3m + 2 \leq r \leq n - 2m + 1, \\ 2n - 2m + 4 - r & \text{if } n - 2m + 2 \leq r \leq n - m + 1, \\ n - 2m + 2 & \text{if } r = n - m + 2, \\ n + 3 - r & \text{if } n - m + 3 \leq r \leq n + 2. \end{cases}$$

It is helpful to organize the strings of β'_q in *ribbons* of parallel strings: the 5 cases of (2) yield, in order:

- A ribbon of width $n - 3m + 1$ which moves m places to the right.
- A ribbon of width m which moves $m + 1$ places to the right, thus leaving the target in position $n - 2m + 2$ unassigned.
- A ribbon of width m which is sent to the final m target positions with a half twist.
- A ‘rogue’ string, which ends at the unassigned target in position $n - 2m + 2$.
- A ribbon of width m , which is sent to the first m target positions with a half twist.

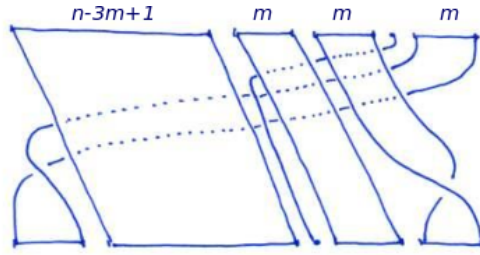


FIGURE 3. The braid $\beta'_{m/n} \in B_{n+2}$.

Definition 3 (The braids β_q). It will be convenient for us to conjugate the braids β'_q by a half twist of the final m strings, thereby turning the half twist on the final ribbon into a full twist, and removing the half twist on the penultimate ribbon: these conjugated braids will be denoted β_q (Figure 4). (The braids β_q can be seen as circular braids, as shown on the right of the figure, with each string other than the rogue one rotating around the circle by either m or $m + 1$ positions. This point of view motivates constructions later in the paper — see Definitions 6 and 10.)

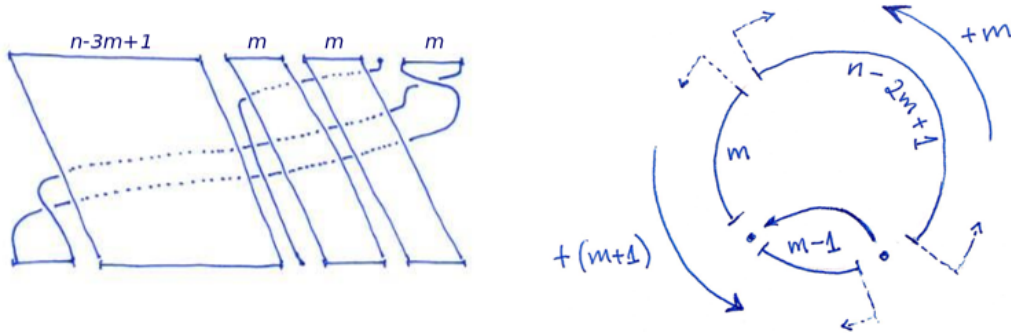


FIGURE 4. The braid $\beta_{m/n} \in B_{n+2}$, and as a circular braid.

3. PSEUDO-ANOSOV CONVERGENCE TO THE TIGHT HORSESHOE

The tight horseshoe map [8] $\varphi_0: S \rightarrow S$ is a 2-sphere homeomorphism which can be obtained by collapsing the horizontal and vertical gaps in the invariant Cantor set of Smale’s horseshoe map [21]. In order to define it directly, we start with its sphere S of definition, which is obtained by making identifications along the sides of a unit square Σ as depicted in Figure 5. Infinitely many segments along the boundary of Σ , two of length $1/2^i$ for each $i \geq 0$, are folded in half (so that the points of each segment, other than the center point, are identified in pairs). The top and right edges of Σ are each a single folded segment, and the other segments are arranged on the left and bottom sides in decreasing order of length from the top left and bottom right vertices respectively. The fold segment endpoints, together with the bottom left corner, are identified to a single point ∞ . It can be shown (see for example [10]) that the space S so obtained is a topological

sphere (and, in fact, that the Euclidean structure on Σ induces a well defined conformal structure on S).

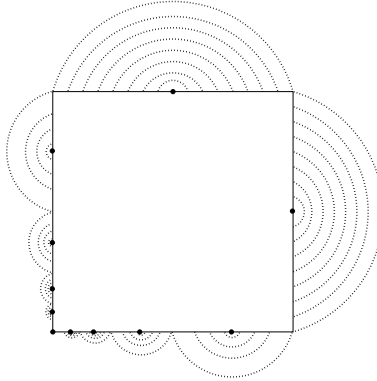


FIGURE 5. The sphere S of definition of the tight horseshoe map.

To define the tight horseshoe map, let $F: \Sigma \rightarrow \Sigma$ be the (discontinuous and non-injective) map defined by

$$F(x, y) = \begin{cases} (2x, y/2) & \text{if } x \leq 1/2, \\ (2 - 2x, 1 - y/2) & \text{if } x > 1/2. \end{cases}$$

That is, F stretches Σ by a factor 2 horizontally, contracts it by a factor 1/2 vertically, and maps its left half to its bottom half, and its right half, with a flip, to its top half. The identifications on Σ are precisely those needed to make F continuous and injective, so that it defines a homeomorphism $\varphi_0: S \rightarrow S$, the tight horseshoe map. (It is an example of a *generalized pseudo-Anosov map* [9]: it has (horizontal and vertical) unstable and stable invariant foliations, but these foliations have infinitely many 1-pronged singularities — at the centers of the fold segments — accumulating on an ‘ ∞ -pronged singularity’ corresponding to the fold segment endpoints and the bottom left vertex.)

For each $q = m/n \in (0, 1/3] \cap \mathbb{Q}$, let $\varphi_q: S^2 \rightarrow S^2$ be a pseudo-Anosov homeomorphism in the mapping class of the $(n + 3)$ -marked sphere defined by β_q . The convergence of φ_q to φ_0 as $q \rightarrow 0$ is an immediate consequence of results from [5]. The following statement is a summary of the relevant parts of theorems 5.19 and 5.31 of that paper.

Theorem 4. *There is a continuously varying family $\{\chi_t: S^2 \rightarrow S^2\}_{t \in (\sqrt{2}, 2]}$ of homeomorphisms of the standard 2-sphere, with the properties that:*

- (a) χ_2 is topologically conjugate to φ_0 ; and
- (b) there is a decreasing function $t: (0, 1/3] \cap \mathbb{Q} \rightarrow (\sqrt{2}, 2)$, satisfying $t(q) \rightarrow 2$ as $q \rightarrow 0$, such that $\chi_{t(q)}$ is topologically conjugate to φ_q for each q .

Remark 5. A brief discussion of the ideas surrounding Theorem 4 may be helpful to the reader. Boyland [4] defined the *braid type* of a period n orbit P of an orientation-preserving disk homeomorphism $f: D^2 \rightarrow D^2$ to be the isotopy class of $f: D^2 \setminus P \rightarrow D^2 \setminus P$, up to conjugacy in the mapping class group of the n -punctured disk: the braid type can therefore be described — although not uniquely — by a braid $\beta_P \in B_n$. He further defined the *forcing relation*, a partial order on the set of braid types: one braid type forces another if every homeomorphism which has a periodic orbit of

the former braid type also has one of the latter. The forcing relation therefore describes constraints on the order in which periodic orbits can appear in parameterized families of homeomorphisms.

If f is Smale's horseshoe map, then standard symbolic techniques associate a *code* $c_P \in \{0, 1\}^n$ to a period n orbit P . This coding establishes a correspondence between the non-trivial periodic orbits of f and those of the affine unimodal *tent maps* $T_t: [0, 1] \rightarrow [0, 1]$ defined for $t \in (1, 2]$ by

$$T_t(x) = \min(2 + t(x - 1), t(1 - x)),$$

whose periodic orbits are likewise coded in a standard way. The braids β'_q of Definition 2 — or, more accurately, the braids β'_q for $q \in (0, 1/2) \cap \mathbb{Q}$ alluded to before the definition — are precisely the pseudo-Anosov braids describing braid types of horseshoe periodic orbits P_q which are *quasi-one-dimensional*, in the sense that the braid types that they force are exactly those corresponding to the periodic orbits of the tent map $T_{t(q)}$ which has kneading sequence $c_{P_q}^\infty$ [15].

Another way to view the braids β'_q is as the braids of horseshoe periodic orbits P_q whose mapping class is pseudo-Anosov and whose associated train tracks are the simplest possible: if the 1-gons about the orbit points are ignored, then the union of the remaining edges is an arc. This means that the only singularities of the invariant foliations of φ_q are 1-prongs at points of the orbit and an n -prong at ∞ , where $q = m/n$. This is what makes the orbits P_q quasi-one-dimensional: the induced map on the train track (which is an interval) is a unimodal interval map.

One way to construct the pseudo-Anosov map in a mapping class is as a factor of the natural extension of a corresponding train track map. In [5], a similar method is used to construct a *measurable pseudo-Anosov* homeomorphism from the natural extension of each tent map T_t with $t > \sqrt{2}$: these form the continuously varying family χ_t of Theorem 4. They are pseudo-Anosov maps if and only if the kneading sequence of the tent map is periodic and is the horseshoe code of one of the braids β'_q , i.e., if and only if $t = t(q)$ for some $q \in (0, 1/2) \cap \mathbb{Q}$, and in this case $\chi_{t(q)}$ is topologically conjugate to φ_q .

Theorem 4 also provides limits of the pseudo-Anosov homeomorphisms φ_q as q tends to an irrational ξ , or to a rational r either from above or from below (the image of t is discrete). All such limits are generalized pseudo-Anosov homeomorphisms.

4. CONVERGENCE OF MAPPING TORI

Let $\nu = \ell/m \in [0, 1) \cap \mathbb{Q}$, and consider the corresponding sequence $(q_k^{(\nu)})_{k \geq 3}$ of rationals defined by $q_k^{(\nu)} = \frac{m}{km + \ell}$. By the description of the ribbon structure of the braids β_q in Section 2, the braid $\beta_{q_k^{(\nu)}}$ is as depicted in Figure 4, with the first ribbon having width $(k - 3)m + \ell + 1$ and the others having width m .

In this section we will show that, for each ν , the mapping tori $M_{q_k^{(\nu)}}$ converge geometrically as $k \rightarrow \infty$ to a hyperbolic manifold \widehat{M}_ν of finite volume. In the following section, we will prove that the set $\{\widehat{M}_\nu: \nu \in [0, 1) \cap \mathbb{Q}\}$ is infinite.

The crucial observation is that the sequence of mapping tori $M_{q_k^{(\nu)}}$ can be obtained from a single finite-volume hyperbolic 3-manifold \widehat{M}_ν by Dehn filling one of its cusps with a sequence of distinct surgery coefficients r_k : it therefore follows from Theorem 1 that the sequence of mapping tori converges geometrically to \widehat{M}_ν .

The manifolds \widehat{M}_ν are themselves mapping tori, corresponding to braids γ_ν which are obtained from $\beta_{q_3^{(\nu)}} = \beta_{m/(3m+\ell)}$ by adding one additional string on the left.

Definition 6 (The braids γ_ν). Let $\nu = \ell/m \in [0, 1) \cap \mathbb{Q}$. The braid $\gamma_\nu \in B_{3m+\ell+3}$ is obtained from $\beta_{m/(3m+\ell)}$ by adding a fixed string on the left, which links with the final width m ribbon of $\beta_{m/(3m+\ell)}$ but not with the other strings, as depicted in Figure 6. (In the circular representation of Figure 4, this corresponds to adding a fixed string, not linking the rogue string, through the center of the circle.)

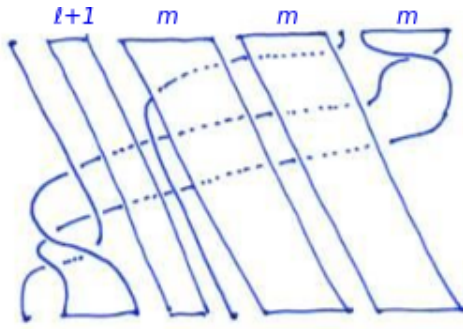


FIGURE 6. The braid $\gamma_{\ell/m}$.

That γ_ν is a pseudo-Anosov braid follows from the fact that $\beta_{m/(3m+\ell)}$ is. (Any reducing curve C would bound a disk D containing at least two but not all of the punctures associated with the strings of γ_ν . D cannot contain the puncture associated to the fixed string, since then its image would also contain that puncture but a different set of the other punctures; it cannot contain a proper subset of the other punctures, since then $\beta_{m/(3m+\ell)}$ would be reducible; and it cannot contain all of the other punctures since the associated strings link with the fixed string.) Therefore $\widehat{M}_\nu := S^3 \setminus (\overline{\gamma}_\nu \cup A)$ (where A is the braid axis) is a finite volume hyperbolic 3-manifold with 3 cusps.

Theorem 7. Let $\nu \in [0, 1) \cap \mathbb{Q}$ and $k \geq 1$. Dehn filling the cusp of \widehat{M}_ν corresponding to the fixed string of γ_ν with surgery coefficient $1/k$ yields $M_{q_{k+3}^{(\nu)}}$.

Proof. It is immediate from Figure 2 that performing a $-k$ twist on the component R of $\overline{\gamma}_\nu \cup A$ corresponding to the fixed string increases the width of the first ribbon of γ_ν from $\ell+1$ to $k\ell+1$. By (1), this changes the surgery coefficient on R to $r_1(R) = 1/(-k + 1/(1/k)) = \infty$, so that it can be erased, yielding the closure of the braid $\beta_{m/((k+3)m+\ell)} = \beta_{q_{k+3}^{(\nu)}}$ (see Figure 4). That is, Dehn filling R with surgery coefficient $1/k$ yields $M_{q_{k+3}^{(\nu)}}$ as required. \square

The following corollary is now immediate from Theorem 1.

Corollary 8. For each $\nu \in [0, 1) \cap \mathbb{Q}$ the sequence $M_{q_k^{(\nu)}}$ converges geometrically to \widehat{M}_ν .

5. INFINITELY MANY LIMIT MANIFOLDS

Figure 7 is a plot of the volumes of the limit manifolds \widehat{M}_ν against ν , generated by SnapPy [7]. The points in red are those for which ν is of the form $k/(k+1)$. In this section we show how all of the corresponding manifolds $\widehat{M}_{k/(k+1)}$ can be obtained by Dehn filling a cusp of another hyperbolic 3-manifold M with a sequence of distinct surgery coefficients, so that, again by Theorem 1, there are infinitely many distinct limit manifolds $\widehat{M}_{k/(k+1)}$ (which converge geometrically to M as $k \rightarrow \infty$).

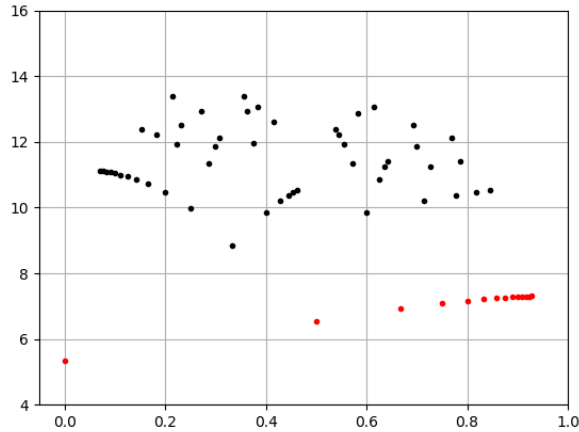
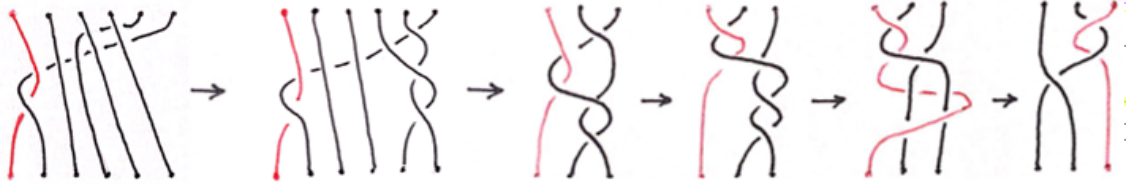


FIGURE 7. Volumes of the limit manifolds \widehat{M}_ν (for ν with denominator ≤ 14).

Remarks 9.

- (a) Other apparently convergent sequences in Figure 7 correspond to similar sequences ν_k , such as $\nu_k = 1/k$ and $\nu_k = k/(2k+1)$.
- (b) The volume $5.333489\dots$ of \widehat{M}_0 suggests that it may be the magic manifold. To see that this is indeed the case, consider the braids depicted in Figure 8, each representing the 3-manifold obtained by removing the braid closure together with its axis from S^3 . The braid on the left is $\gamma_{0/1}$, representing \widehat{M}_0 , while the one on the right represents the magic manifold (see for example Figure 3 of [16]). The operations converting each braid to the next are either twists on components of the associated links or braid conjugacies, and therefore leave the 3-manifolds unchanged. Specifically, these operations are, in order: conjugacy by σ_4^{-1} ; a +3 twist on the red component (see Figure 1 (d) and (a)); conjugacy by σ_2 ; a +1 twist on the braid axis; and conjugacy by $\sigma_1\sigma_2$.

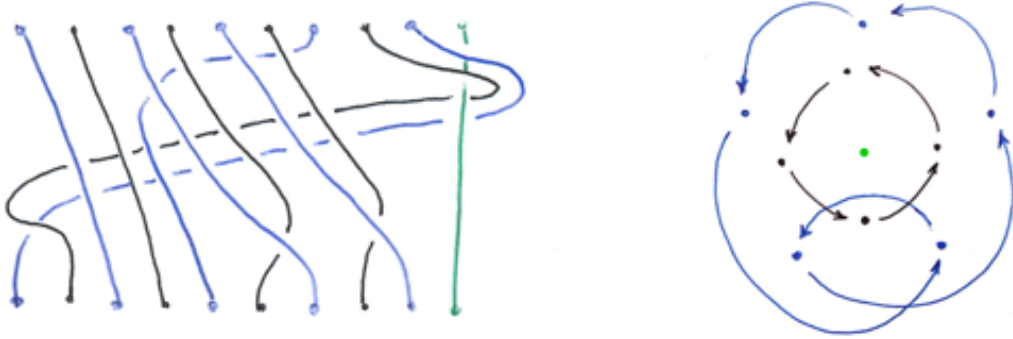
The manifold M is obtained from the 10-braid δ of the following definition (see Figure 9), whose closure $\bar{\delta}$ is a three-component link. Note that the blue and green strings in the figure form a braid conjugate to $\gamma_{0/1}$ (the conjugacy moves the green string from the left to the right of the braid diagram), and to this braid has been added a 4-string braid which ‘shadows’ the blue strings. It is not obvious a priori — at least, not to the authors — that Dehn filling the ‘black’ cusp of the

FIGURE 8. \widehat{M}_0 is the magic manifold.

resulting hyperbolic 3-manifold should yield the manifolds $\widehat{M}_{k/(k+1)}$: rather, the braid δ was found experimentally using SnapPy [7].

Definition 10. Let $\delta = \sigma_6\sigma_5\sigma_4\sigma_3\sigma_9\sigma_8\sigma_8\sigma_9\sigma_7\sigma_6\sigma_5\sigma_4\sigma_3\sigma_2\sigma_1\sigma_8\sigma_7\sigma_6\sigma_5\sigma_4\sigma_3\sigma_2\sigma_1\sigma_8\sigma_6 \in B_{10}$.

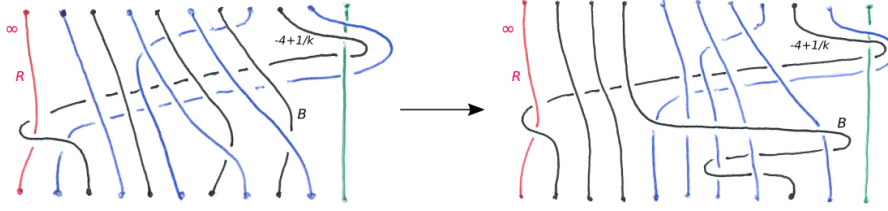
It can be checked (for example, using a train track algorithm such as the one due to Bestvina and Handel [2]) that δ is pseudo-Anosov: the corresponding relative pseudo-Anosov homeomorphism has 1-pronged singularities at the marked points corresponding to the blue and green strings of Figure 9, a 4-pronged singularity at ∞ , and regular points at the black marked points. Therefore $M := S^3 \setminus (\bar{\delta} \cup A)$ (where A is the braid axis) is a finite volume hyperbolic 3-manifold with 4 cusps.

FIGURE 9. The braid $\delta \in B_{10}$.

Theorem 11. Let $k \geq 1$. Dehn filling the cusp of M corresponding to the black strings of Figure 9 with surgery coefficient $-4 + 1/k$ yields $\widehat{M}_{k/(k+1)}$.

Proof. The left hand side of Figure 10 depicts a braid ζ , which is δ together with an extra fixed string shown in red. We write B and R for the black and red components of $\bar{\zeta}$, which are unknotted. We need to show that filling B with coefficient $r_0(B) = -4 + 1/k$ and R with coefficient $r_0(R) = \infty$ (i.e. erasing R from the link $\bar{\zeta} \cup A$) yields the 3-manifold $\widehat{M}_{k/(k+1)}$.

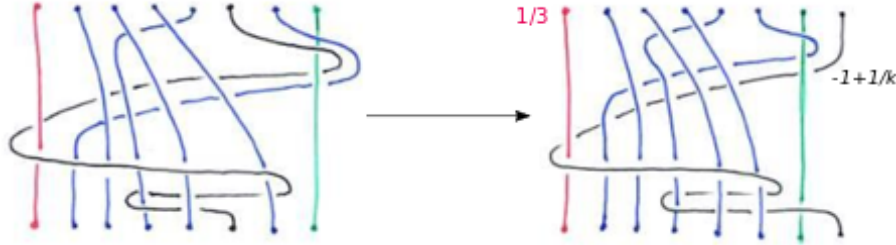
The braid on the right hand side of the figure is obtained by conjugating by $\sigma_7^{-2}\sigma_2^{-1}\sigma_4^{-1}\sigma_3^{-1}\sigma_6^{-1}\sigma_5^{-1}\sigma_4^{-1}$. Referring to Figure 1, performing a +3 twist on R yields the braid on the left of Figure 11, and a conjugacy by $\sigma_6^{-1}\sigma_7$ gives the braid on the right hand side of the figure. By (1), the updated


 FIGURE 10. Conjugating ζ to prepare it for a $+3$ twist on R .

surgery coefficients are:

$$\begin{aligned} r_1(R) &= 1/(3 + 1/r_0(R)) = 1/3, \text{ and} \\ r_1(B) &= r_0(B) + 3 = -1 + 1/k, \end{aligned}$$

since $\text{lk}(B, R) = 1$.


 FIGURE 11. A $+3$ twist on R , followed by a conjugacy.

Performing a $+1$ twist on the braid axis A yields the braid on the left hand side of Figure 12, which a further conjugacy by $\sigma_7\sigma_6\sigma_5\sigma_4\sigma_3\sigma_2\sigma_1\sigma_1\sigma_2\sigma_3\sigma_4\sigma_5\sigma_6\sigma_7$ — to pull the black string around — reduces to the right hand side of the figure. (Here and in Figure 13, the parts of the blue strings which participate in the full twist have not been drawn, to clarify the diagrams.) The red component R and the black component B are now unlinked. The revised surgery coefficients are

$$\begin{aligned} r_2(R) &= 1/3 + 1 = 4/3, \text{ and} \\ r_2(B) &= -1 + 1/k + 1 = 1/k, \end{aligned}$$

since $\text{lk}(A, R) = \text{lk}(A, B) = 1$.

We can now carry out the surgery on B . Performing a $-k$ twist on B yields the braid of Figure 13 (in which the ribbon contains $k - 1$ parallel strings). The surgery coefficient of B is

$$r_3(B) = \frac{1}{-k + 1/(1/k)} = \infty,$$

so that it can be removed (and is not shown in Figure 13). Because R and B are unlinked, the surgery coefficient of R is unchanged: $r_3(R) = r_2(R) = 4/3$.

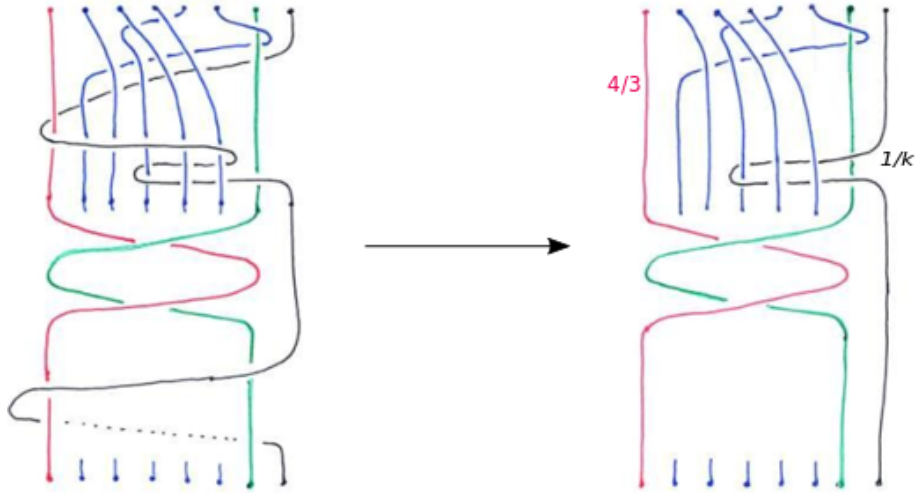


FIGURE 12. A $+1$ twist on the braid axis A , followed by a conjugacy.

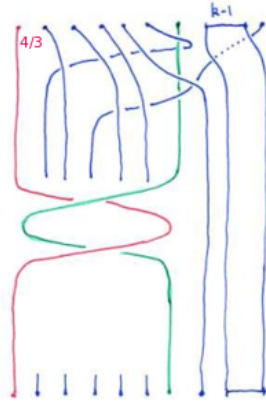


FIGURE 13. A $-k$ twist on B changes its surgery coefficient to ∞ .

We next perform a -1 twist on A , which produces the braid on the left hand side of Figure 14, and changes the surgery coefficient of R to $r_4(R) = 1/3$. A -3 twist on R therefore changes its coefficient to ∞ , so that it can be erased: this results in the braid on the right hand side of Figure 14, in which each of the four ribbons contains $k - 1$ parallel strings.

To complete the proof, we exhibit a braid conjugacy between the braid on the right hand side of Figure 14 and the braid $\gamma_{k/(k+1)}$ — that is, the braid of Figure 6 with all four ribbons containing $k + 1$ parallel strings. (This conjugacy was discovered computationally, using sliding circuit set methods [13, 14] for small values of k and extrapolating: the braids $\gamma_{k/(k+1)}$ have small sliding circuit sets but large ultra summit sets [12].) Two successive conjugacies are shown in

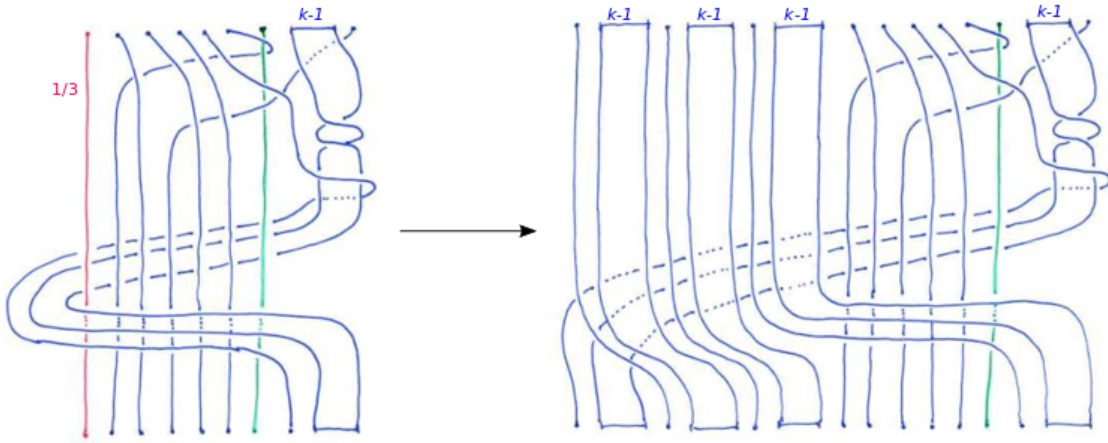


FIGURE 14. A -1 twist on A followed by a -3 twist on R .

Figure 15. Here the first, second, and fourth ribbons have been enlarged by incorporating an additional parallel string, so that they each contain k parallel strings.

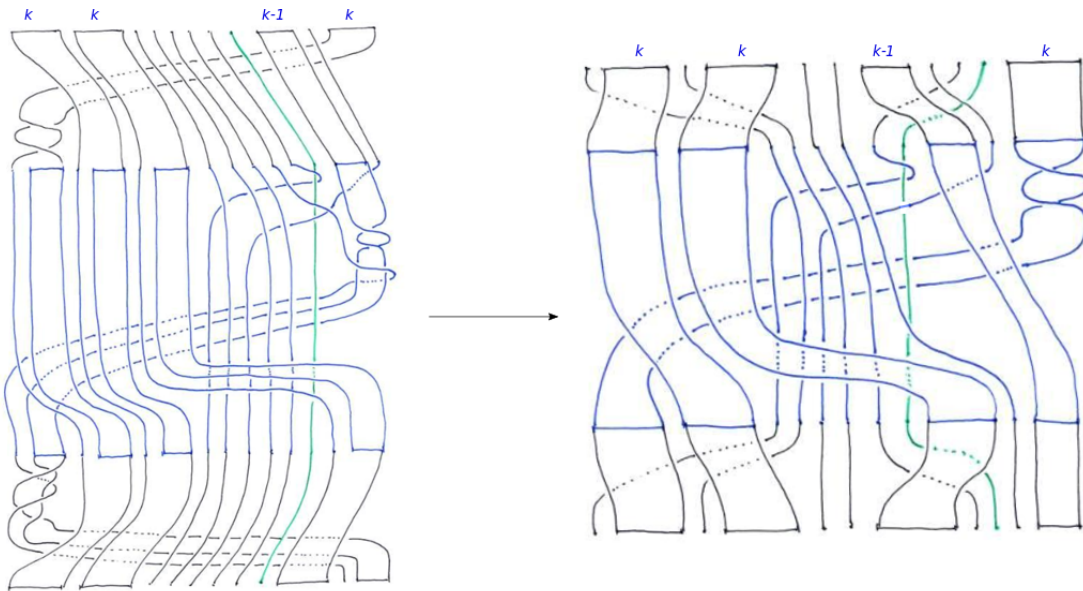


FIGURE 15. Successive conjugacies on the right hand side of Figure 14.

Simplifying the braid on the right hand side of Figure 15 by isotopy of the strings yields the braid on the left hand side of Figure 16. Again, we have incorporated additional parallel strings into ribbons, so that the first two ribbons contain $k + 1$ parallel strings, and the other two contain k parallel strings. A final conjugacy which moves the green string to the left, underneath all of the

other strings, gives the braid on the right hand side of the figure, and incorporating additional parallel strings into the rightmost two ribbons yields $\gamma_{k/(k+1)}$ as required.

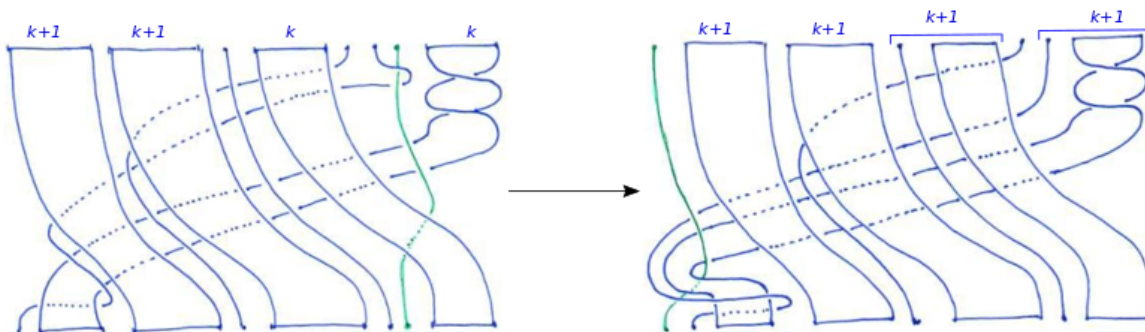


FIGURE 16. A simplified diagram of the right hand side of Figure 15, followed by a conjugacy.

□

Corollary 12. *The sequence $\widehat{M}_{k/(k+1)}$ converges geometrically to M as $k \rightarrow \infty$, and there are infinitely many distinct hyperbolic 3-manifolds $\widehat{M}_{k/(k+1)}$.*

REFERENCES

1. R. Benedetti and C. Petronio, *Lectures on hyperbolic geometry*, Universitext, Springer-Verlag, Berlin, 1992. MR 1219310
2. M. Bestvina and M. Handel, *Train-tracks for surface homeomorphisms*, *Topology* **34** (1995), no. 1, 109–140. MR 1308491
3. J. Birman, *Braids, links, and mapping class groups*, Princeton University Press, Princeton, N.J., 1974, Annals of Mathematics Studies, No. 82. MR 0375281
4. P. Boyland, *Topological methods in surface dynamics*, *Topology Appl.* **58** (1994), no. 3, 223–298. MR 1288300
5. P. Boyland, A. de Carvalho, and T. Hall, *Natural extensions of unimodal maps: virtual sphere homeomorphisms and prime ends of basin boundaries*, arXiv:1704.06624v2 [math.DS] (2018).
6. A. Casson and S. Bleiler, *Automorphisms of surfaces after Nielsen and Thurston*, London Mathematical Society Student Texts, vol. 9, Cambridge University Press, Cambridge, 1988. MR 964685
7. M. Culler, N. Dunfield, M. Goerner, and J. Weeks, *SnapPy, a computer program for studying the geometry and topology of 3-manifolds*, Available at <http://snappy.computop.org> [downloaded: 20/12/18], 2018.
8. A. de Carvalho, *Extensions, quotients and generalized pseudo-Anosov maps*, *Graphs and patterns in mathematics and theoretical physics*, Proc. Sympos. Pure Math., vol. 73, Amer. Math. Soc., Providence, RI, 2005, pp. 315–338. MR 2131019
9. A. de Carvalho and T. Hall, *Unimodal generalized pseudo-Anosov maps*, *Geom. Topol.* **8** (2004), 1127–1188. MR 2087080
10. ———, *Paper folding, Riemann surfaces and convergence of pseudo-Anosov sequences*, *Geom. Topol.* **16** (2012), no. 4, 1881–1966. MR 2975296
11. A. Fathi, F. Laudenbach, and V. Poénaru, *Travaux de Thurston sur les surfaces*, Astérisque, vol. 66, Société Mathématique de France, Paris, 1979, Séminaire Orsay, With an English summary. MR 568308
12. V. Gebhardt, *A new approach to the conjugacy problem in Garside groups*, *J. Algebra* **292** (2005), no. 1, 282–302. MR 2166805
13. V. Gebhardt and J. González-Meneses, *The cyclic sliding operation in Garside groups*, *Math. Z.* **265** (2010), no. 1, 85–114. MR 2606950

14. ———, *Solving the conjugacy problem in Garside groups by cyclic sliding*, J. Symbolic Comput. **45** (2010), no. 6, 629–656. MR 2639308
15. T. Hall, *The creation of horseshoes*, Nonlinearity **7** (1994), no. 3, 861–924.
16. E. Kin and M. Takasawa, *Pseudo-Anosovs on closed surfaces having small entropy and the Whitehead sister link exterior*, J. Math. Soc. Japan **65** (2013), no. 2, 411–446. MR 3055592
17. C. McMullen, *Renormalization and 3-manifolds which fiber over the circle*, Annals of Mathematics Studies, vol. 142, Princeton University Press, Princeton, NJ, 1996. MR 1401347
18. W. Neumann and D. Zagier, *Volumes of hyperbolic three-manifolds*, Topology **24** (1985), no. 3, 307–332. MR 815482
19. J-P. Otal, *The hyperbolization theorem for fibered 3-manifolds*, SMF/AMS Texts and Monographs, vol. 7, American Mathematical Society Providence RI; Société Mathématique de France Paris, 2001, Translated from the 1996 French original by Leslie D. Kay. MR 1855976
20. D. Rolfsen, *Knots and links*, Mathematics Lecture Series, vol. 7, Publish or Perish Inc., Houston TX, 1990, Corrected reprint of the 1976 original. MR 1277811
21. S. Smale, *Differentiable dynamical systems*, Bull. Amer. Math. Soc. **73** (1967), 747–817. MR 0228014
22. W. Thurston, *On the geometry and dynamics of diffeomorphisms of surfaces*, Bull. Amer. Math. Soc. (N.S.) **19** (1988), no. 2, 417–431. MR 956596
23. ———, *Hyperbolic structures on 3-manifolds, II: surface groups and 3-manifolds which fiber over the circle*, arXiv:9801045v1 [math.GT] (1998).
24. ———, *The geometry and topology of three-manifolds*, Available at <http://library.msri.org/books/gt3m/> [downloaded: 20/12/18], 2002.

DEPARTAMENTO DE MATEMÁTICA, IME-USP, RUA DO MATÃO 1010, CIDADE UNIVERSITÁRIA, 05508-090 SÃO PAULO SP, BRAZIL

E-mail address: `sylvain@ime.usp.br`

DEPARTAMENTO DE MATEMÁTICA APLICADA, IME-USP, RUA DO MATÃO 1010, CIDADE UNIVERSITÁRIA, 05508-090 SÃO PAULO SP, BRAZIL

E-mail address: `andre@ime.usp.br`

DEPARTAMENTO DE ÁLGEBRA, INSTITUTO DE MATEMÁTICAS (IMUS), UNIVERSIDAD DE SEVILLA, AV. REINA MERCEDES S/N, 41012 SEVILLA, SPAIN

E-mail address: `meneses@us.es`

DEPARTMENT OF MATHEMATICAL SCIENCES, UNIVERSITY OF LIVERPOOL, LIVERPOOL L69 7ZL, UK

E-mail address: `tobyhall@liverpool.ac.uk`